Smith, E. L., Landon, M., Piszkiewicz, D., Brattin, W. J., Langley, J. J., & Malamed, M. D. (1970) *Proc. Natl. Acad. Sci. U.S.A. 67*, 724–730.

Stryer, L. (1978) *Annu. Rev. Biochem. 47*, 819–846.

Sund, H., Markau, K., & Koberstein, R. (1975) *Biol. Macromol.* 225–287.

Tomich, J. M., Marti, C., & Colman, R. F. (1981) *Biochemistry 20*, 6711–6720.

Conformational Changes of Adrenocorticotropin Peptides upon Interaction with Lipid Membranes Revealed by Infrared Attenuated Total Reflection Spectroscopy†

Hans-Ulrich Gremlich,* Urs-Peter Fringeli, and Robert Schwyzer

ABSTRACT: Infrared attenuated total reflection (IR-ATR) spectroscopy was used to study conformational and topological aspects of the interaction between two adrenocorticotropin fragments and dioleoylphosphatidylcholine membranes. Corticotropin-(1–10)-decapeptide, $ACTH_{1-10}$, was found to exist as a rigid antiparallel pleated sheet structure in dry membranes. In aqueous environment, it completely escaped from the lipid. This dominant preference for the aqueous phase is a possible explanation for the very low biological potency of $ACTH_{1-10}$ in some assays. On the other hand, the very potent corticotropin-(1–24)-tetracosapeptide, $ACTH_{1-24}$, was firmly incorporated into dry and wet membranes. Aqueous environment even promoted the peptide–lipid interaction. Under these latter conditions, part of the molecule entered the bilayer and adopted a helical structure with the axis oriented perpendicularly to the bilayer plane. Contact of a 0.1 mM solution of $ACTH_{1-24}$ in liquid deuterium oxide with the pure lipid membrane system resulted in measurable adsorption of the peptide to the membrane with the same conformational and topological characteristics as described above (perpendicularly oriented helix entering the bilayer). The helical part of the $ACTH_{1-24}$ molecule entering the bilayer was the quite hydrophobic N-terminal decapeptide unit ("message" segment). The adjacent hydrophilic C-terminal tetradecapeptide unit ("address" segment) remained on the membrane surface. As the message region is essential for triggering corticotropin receptors, its intrusion into the membrane and its adoption of an oriented, helical conformation may facilitate receptor stimulation. Our experiments clearly demonstrate that the observed specific membrane interaction critically depended on the presence of the address segment. This could explain the potentiating effect of the "address" in pharmacological experiments.

Adrenocorticotrophic hormone (adrenocorticotropin, corticotropin, ACTH;[1] Table I) is a linear nonatriacontapeptide elaborated in the anterior lobe of the pituitary gland and in certain regions of the brain [for recent reviews, see Schwyzer (1977, 1982)]. ACTH acts on the adrenal cortex, the skin, and the central nervous system, causing steroidogenesis, melanophore darkening, and behavioral changes, respectively. It exerts its effects through saturable and reversible interactions with specific receptors contained in the outer membranes of its target cells [see Schulster & Schwyzer (1980)].

Synthetic N-terminal segments of ACTH are found to be responsible for the hormonal activity and to have specific receptor binding properties (Schwyzer et al., 1960; Lang et al., 1974). Thus, adrenocorticotropin-(1–24)-tetracosapeptide ($ACTH_{1-24}$; Schwyzer & Kappeler, 1963) is a fully potent full agonist of established therapeutic value. Adrenocorticotropin-(1–10)-decapeptide ($ACTH_{1-10}$) is also a full agonist, but with very low potency in adrenal cells (10^{-6}–10^{-5} × [$ACTH_{1-24}$]; Schwyzer et al., 1971), low potency in melanophores (about 10^{-2} × [$ACTH_{1-24}$]; Eberle & Schwyzer, 1976), and high potency (equal to [$ACTH_{1-24}$]; de Wied et al., 1975) in a behavioral assay. Adrenocorticotropin-(11–24)-tetradecapeptide is an antagonist for steroidogenesis (Seelig et al., 1971) without any agonist properties in this and the other two assays. It is concluded that segment 1–10 of $ACTH_{1-24}$ carries the message for triggering the receptor response and that segment 11–24 modulates the potency of the message segment with respect to different receptors (address function) [see Schwyzer (1977)]. The molecular mechanism responsible for the drastic potentiation of the message by the address in the adrenal cell response is unknown: Enhancement of specific affinity for the receptor through additional, specific binding energy between address and re-

Table I: Primary Structure of Adrenocorticotrophic Hormone of Human Origin at Neutral pH

```
(+) Ser-Tyr-Ser-Met-Glu(–)-His-Phe-Arg(+)-Trp-Gly-Lys(+)-Pro-
     1               5                        10
Val-Gly-Lys(+)-Lys(+)-Arg(+)-Arg(+)-Pro-Val-Lys(+)-Val-Tyr-
        15                          20
Pro-Asn-Gly-Ala-Glu(–)-Asp(–)-Glu(–)-Ser-Ala-Glu(–)-Ala-Phe-Pro-
24  25                        30                            35
Leu-Glu(–)-Phe(–)
           39
```

† From the Departments of Molecular Biology and Biophysics (H.-U.G. and R.S.) and Physical Chemistry (U.-P.F.), Swiss Federal Institute of Technology (ETH), CH-8093 Zürich, Switzerland. *Received February 4, 1983.* Supported by project funds of the ETH and the Swiss National Science Foundation. Dedicated to the memory of Ernesto Scoffone, Padova.

[1] Abbreviations: ACTH, adrenocorticotrophic hormone; $ACTH_{n-m}$, synthetic ACTH peptides comprising the amino acid residues *n–m* of the natural sequence; IR-ATR, infrared attenuated total reflection.

0006-2960/83/0422-4257$01.50/0

ceptor is one possibility; favorable influences on the conformation of the message in certain surroundings (cell surface) another [see Seelig et al. (1971) and Schwyzer (1977)].

The lipid phase of the target cell membrane acts as a matrix for the receptors: it is essential for the functionality and the correct topological arrangement of the receptor proteins [see Sonenberg & Schneider (1977)]. We wondered whether the lipid phase might also be, at least partly, responsible for the proper function of the $ACTH_{1-24}$ molecule. The lipid phase might conceivably influence the receptor interaction by an antennae-like capture of the peptide from the surrounding fluid [as theoretically postulated by Adam & Delbrück (1968) and by Berg & Purcell (1977)] and by inducing peptide conformations and topological arrangements prior to and in a manner favorable for the receptor interaction.

Indeed, the absorption of $ACTH_{1-24}$ to lipid bilayer membranes, as measured by capacitance minimization (Gremlich et al., 1981), is found to be large enough to make capture and, hence, reduction of the dimensionality of diffusion (Adam & Delbrück, 1968) appear to be a preferred molecular process, thus facilitating receptor search by the peptide (requirement of $K_{diss} \leq 6.5 \times 10^{-3}$ M, according to Berg & Purcell (1977)]. We therefore addressed ourselves to the second part of our question: Does the adsorption of $ACTH_{1-24}$ to lipid membranes cause conformational transitions of the peptide molecules and distinct orientations of the peptide with respect to the lipid membrane? [For a preliminary account, see Schwyzer et al. (1983).]

The possibility of conformational transitions within the ACTH molecule is well documented in the literature. According to the classical work of Squire & Bewley (1965), ACTH has a mainly random conformation in aqueous roundings, but a small region close to the N terminus appears to have the tendency to form 1–1.5 turns of a helical structure. Application of the Chou & Fasman (1978) rules indicates a clustering of helix-forming potential in the region of amino acid residues 3–9 (Greff et al., 1976). Circular dichroism (Greff et al., 1976), as well as the qualitative interpretation of infrared spectra and the quantitative analysis of ^1H–^2H exchange data (Nabedryk-Viala et al., 1978), indicates that a transition from a random structure to a predominantly α-helical structure is induced in the N-terminal but not in the C-terminal part of the $ACTH_{1-24}$ by changing the solvent from water to trifluoroethanol. Trifluoroethanol is considered to promote conformational transitions in peptides and proteins that are comparable to those caused by an approach of membrane surroundings (Pitner & Urry, 1972). The α-helical structure of the segment encompassing residues 3–9 in trifluoroethanol solutions of $ACTH_{1-32}$, $ACTH_{1-19}$, and $ACTH_{1-14}$ is demonstrated by nuclear magnetic resonance and circular dichroism (Toma et al., 1981). Information on $ACTH_{1-10}$ is lacking, but $ACTH_{5-10}$ is not prone to a random coil–helix transition on going from water to trifluoroethanol (Greff et al., 1976).

In addition to such site-specific conformational transitions in the isotropic and symmetrical surroundings provided by water and trifluoroethanol, orientational and perhaps different conformational effects might be induced in the asymmetric and anisotropic surroundings provided by the liquid-crystalline ultrastructure of lipid bilayer membranes. We investigated these possibilities by the powerful and yet relatively simple technique of infrared attenuated total reflection spectroscopy (Harrick, 1967) as applied to lipid membranes by Fringeli (1977) and Fringeli & Günthard (1981). We concentrated our attention on the interaction of $ACTH_{1-10}$ and $ACTH_{1-24}$

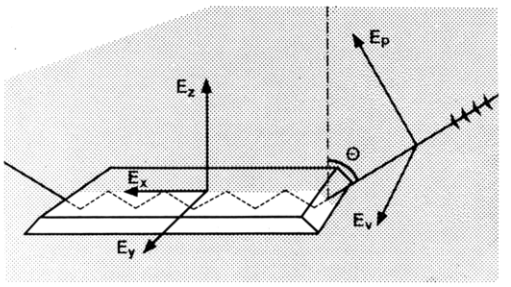

FIGURE 1: ATR setup: θ, angle of incidence; E_p and E_v, parallel and perpendicular polarized components of the electric field of incident light; E_x, E_y, and E_z, electric field components with respect to the coordinate system corresponding to the internal reflection plate ($E_p \rightarrow E_x$ and E_z; $E_v \rightarrow E_y$).

with dioleoylphosphatidylcholine bilayer systems. Discrete conformational transitions, insertions, and orientations with respect to the plane of the membranes were found. These phenomena were critically dependent on membrane hydration, i.e., on the similarity of lipid arrangement in the model membranes to that in biological systems (Fringeli, 1977). Our observations provided significant correlations between the lipid interactions and the pharmacological behavior of the two peptides and their segments. Thus, the strongly charged address segment contained the molecular information necessary for producing the hydrophobic interaction, the conformational transition, and the orientation of the message segment in the membranes.

Experimental Procedures

For general information about internal reflection spectroscopy, see Harrick (1967). Details of the application of infrared attenuated total reflection (IR-ATR) spectroscopy to lipid membrane research are given by Fringeli (1977) and Fringeli & Günthard (1981).

IR-ATR spectra were determined with a Perkin-Elmer infrared spectrophotometer 580 equipped with an Interdata Model 6/16 computer, with polished ZnSe crystals as internal reflection plates. All spectra represented in the figures were the means of four scans. The spectral resolution was better than 1.5 cm^{-1} in the amide I region. The abscissa accuracy was always within ± 0.25 cm^{-1}, and the reproducibility of the absorbance was better than 0.002 absorbance unit. Peptide spectra were the difference of the total spectra minus the lipid membrane spectra. They were scanned with parallel (E_p) and perpendicular (vertical, E_v) polarized incident light, Figure 1. Relative to the fixed coordinate system defined by the internal reflection plate, E_p revealed the E_x and E_z components of the IR absorption, whereas E_v revealed its E_y component (Fringeli, 1977; Fringeli & Günthard, 1981). Polarization was expressed as the dichroic ratio $R = A_p/A_v$, where A_v and A_p are the absorbances measured with E_v and E_p, respectively.

The peptides, adrenocorticotropin-(1–10)-decapeptide ($ACTH_{1-10}$) and adrenocorticotropin-(1–24)-tetracosapeptide ($ACTH_{1-24}$), were synthesized according to Schwyzer & Kappeler (1963). 1,2-Dioleoyl-*sn*-glycero-3-phosphocholine (DOPC) was purchased from R. Berchtold (Biochemical Laboratory, CH-3007 Bern). Samples that became oxidized during handling were revealed by their IR absorption at 1645 cm^{-1} [β-diketone ν(C=O)] and were discarded. To measure the spectra of pure peptides without lipid, the compounds were dissolved in methanol, and a few drops of the solutions were spread on the internal reflection plate and evaporated, leaving thin films of the peptide.

For preparing model membranes, peptide and lipid were dissolved in methanol at molar ratios of DOPC to peptide of

Table II: Dichroic Ratio R of $ACTH_{1-10}$ Amide I and Amide II Absorption Bands at 25 °C

sample	$R_{amide\ I}$	$R_{amide\ II}$
$ACTH_{1-10}$	1.1 ± 0.1	1.1 ± 0.1
DOPC/$ACTH_{1-10}$ (50:1)	1.2 ± 0.1	1.5 ± 0.1
DOPC/$ACTH_{1-10}$ (75:1)	1.1 ± 0.1	1.4 ± 0.1
DOPC/$ACTH_{1-10}$ (100:1)	1.1 ± 0.1	1.3 ± 0.1

50:1, 75:1, 100:1, and 120:1. Some drops of the solution to be examined were spread on the two polished surfaces of the ZnSe crystal. *Dry* multibilayers were formed by evaporating the solvent (Fringeli, 1977). Stable, *equilibrated* membranes were obtained by exposure of the dry membranes to liquid water for 20–30 min, followed by drying in a current of nitrogen until the intensity of the water absorption band at 3400 cm^{-1} had diminished to a constant value. Equilibrated DOPC model membranes were multibilayers with an average thickness of five bilayers as estimated from the intensity of the α-methylene bending vibrations of the hydrocarbon chains (Fringeli, 1980). The adsorption of peptides onto preformed, equilibrated membranes of pure DOPC was investigated by contacting the membranes with solutions of peptide in ^2H_2O, because it was difficult exactly to compensate the strong H_2O band at 1645 cm^{-1} that interfered with the peptide amide I absorption.

Deuterium exchange experiments were performed by exposure of the peptide films or the model membranes to an atmosphere of N_2 saturated with ^2H_2O or to liquid ^2H_2O. The rate of ^1H–^2H exchange was estimated semiquantitatively from the reduction of the ν(N–H) absorbance at 3280 cm^{-1}.

Results and Discussion

Spectroscopic Considerations. Our analysis of ACTH peptide secondary structure was based on the examination of the positions and shapes of the amide I [~80% ν(C=O), ~10% ν(C–N), ~10% δ(N–H)], amide II [~60% δ(N–H), ~40% ν(C–N)], and ν(N–H) absorption bands, as the amide-group vibrations critically depend on peptide secondary structure (Miyazawa, 1967; Nabedryk-Viala et al., 1978). The polarizations of the amide group vibrations were used to examine the preferred orientations of regular secondary structures relative to the lipid bilayers. In an α-helix, the main components of the transition dipole moments are parallel (amide I) and perpendicular (amide II) to the helix axis (Nevskaya & Chirgadze, 1976), while in an antiparallel β-pleated sheet, the polarizations are opposite, i.e., predominantly perpendicular (amide I) and parallel (amide II) to the fiber axis (Chirgadze & Nevskaya, 1976).

The conformational assignments were semiquantitatively checked by hydrogen–deuterium exchange, which is definitely slower in ordered regions of ACTH peptides than in unordered ones (Nabedryk-Viala et al., 1978).

Antiparallel β-Pleated Sheet of $ACTH_{1-10}$. IR-ATR spectra between 1700 and 1500 cm^{-1} of pure $ACTH_{1-10}$ are shown in Figure 2a. The absorbance peaks at 1630 and 1695 cm^{-1} indicated the presence of antiparallel β-pleated sheet structures (Chirgadze & Nevskaya, 1976), while the adsorption at 1650 cm^{-1} was characteristic of admixed random structures (Miyazawa, 1967).

The antiparallel β-pleated sheet of $ACTH_{1-10}$ was maintained in dry (unequilibrated) model membranes with DOPC/$ACTH_{1-10}$ molar ratios of 50:1, 75:1, and 100:1 (Figure 2b–d). The relative amount of β-pleated sheet, however, diminished in this dilution series.

The amide I and II bands of pure $ACTH_{1-10}$ had no distinct polarization (Table II). Thus, the β-pleated sheet structures

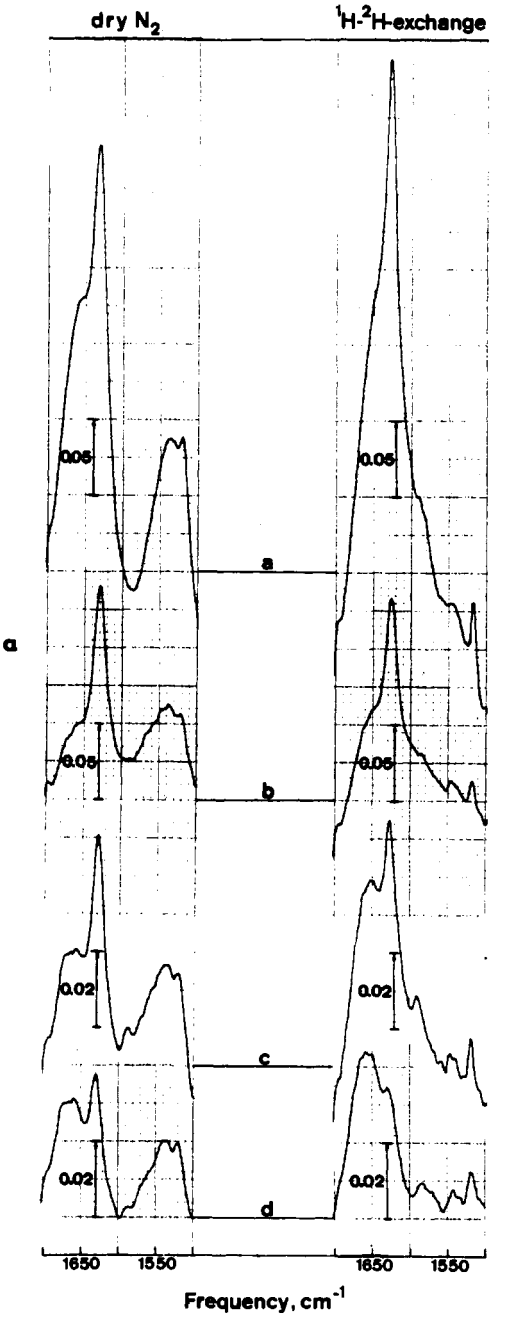

FIGURE 2: Behavior of $ACTH_{1-10}$ in DOPC multilayer membranes reflected by amide I and amide II IR-ATR absorption bands (absorbance plot, $\alpha = -\log T$, in which T is transmittance). Samples were either dried with dry N_2 or flushed with a ^2H_2O-saturated N_2 stream (^1H–^2H exchange) for 16 h. All spectra were recorded with parallel polarized incident light (plane of polarization perpendicular to the plane of the membrane surface). (a) Pure $ACTH_{1-10}$, 25 °C, deposited directly on the ZnSe surface by drying a solution in CH_3OH. (b) Model membrane prepared from CH_3OH solution (5 mM DOPC, 0.1 mM $ACTH_{1-10}$), 25 °C. (c) Model membrane prepared from CH_3OH solution (7.5 mM DOPC, 0.1 mM $ACTH_{1-10}$), 25 °C. (d) Model membrane prepared from CH_3OH solution (10 mM DOPC, 0.1 mM $ACTH_{1-10}$), 25 °C.

of $ACTH_{1-10}$ (or any other regular structures possibly present) showed no preferred orientation on the ZnSe crystals. However, for $ACTH_{1-10}$ in dry, unequilibrated DOPC model membranes, the dichroic ratio of the amide II band was significantly increased, while the amide I band remained unpolarized. Upon dilution of the peptide in the membrane, the dichroic ratio slightly decreased. The polarizations indicated an orientation of the peptide chains perpendicular to the bilayers.

Table III: Hydrogen-Deuterium Exchange of Amide Protons in an Atmosphere of N_2 Saturated with ^2H_2O at 25 °C during 16 h

sample	percent amide protons exchanged
$ACTH_{1-10}$	48 ± 3
$DOPC/ACTH_{1-10}$ (50:1)	42 ± 3
$DOPC/ACTH_{1-10}$ (75:1)	51 ± 3
$DOPC/ACTH_{1-10}$ (100:1)	~60–70

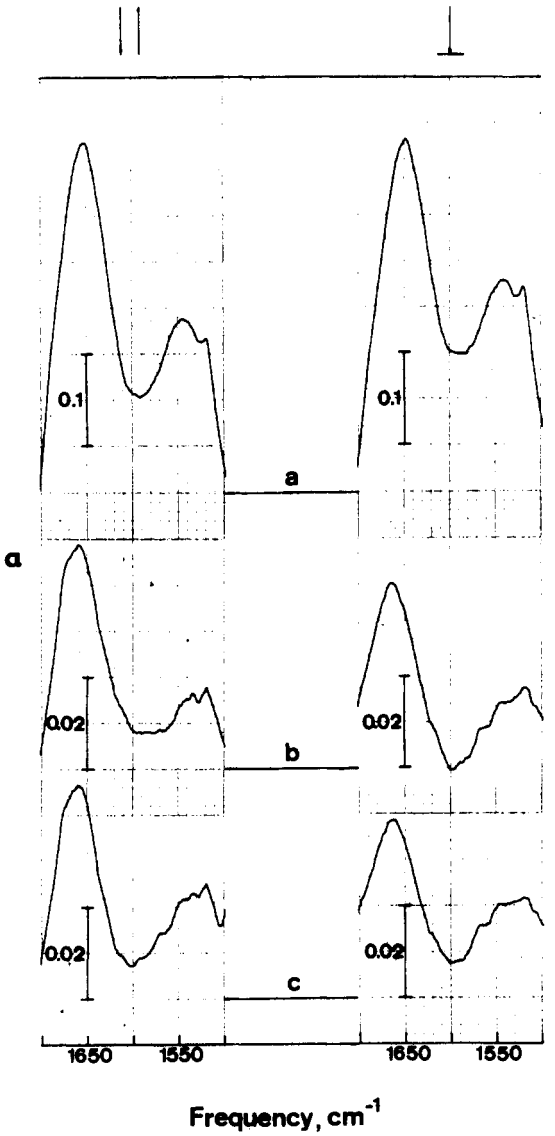

FIGURE 3: Behavior of $ACTH_{1-24}$ in DOPC multilayer membranes reflected by amide I and amide II IR-ATR absorption bands (absorbance plot, $\alpha = -\log T$, in which T is transmittance): ($\parallel$ and $\perp$) parallel and perpendicular polarized incident light, respectively. (a) Pure $ACTH_{1-24}$, dry N_2, 25 °C. (b) Model membrane prepared from CH_3OH solution (7.5 mM DOPC, 0.1 mM $ACTH_{1-24}$), after 20-min contact with liquid H_2O, dry N_2, 25 °C, for adequate drying. Spectra of the pure DOPC membrane have been subtracted. (c) Model membrane prepared from CH_3OH solution (10 mM DOPC, 0.1 mM $ACTH_{1-24}$), after 20-min contact with liquid H_2O, dry N_2, 25 °C, for adequate drying. Spectra of the pure DOPC membrane have been subtracted.

The antiparallel β-pleated sheets of $ACTH_{1-10}$, either in the pure peptide films or in dry, unequilibrated membranes, were rather rigid, as shown by ^1H–^2H exchange (Table III). However, with increasing dilution of $ACTH_{1-10}$ in the membranes, more amide groups became accessible to the exchange reaction. The behavior of the ^1H–^2H exchange, of the dichroic ratios, and of the absorbance indicated that the amount of

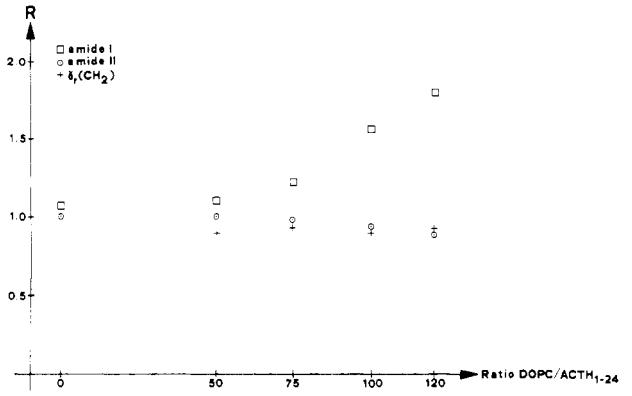

FIGURE 4: Dichroic ratio R for amide I, amide II, and $\gamma_r(CH_2)$ absorption bands in dependence of molar ratios $DOPC/ACTH_{1-24}$. Values obtained from polarization measurements in $DOPC/ACTH_{1-24}$ model membranes after 20-min contact with liquid H_2O, dry N_2, 25 °C, for adequate drying.

β-pleated sheet structures diminished upon dilution of $ACTH_{1-10}$ in the dry model membranes.

Upon moistening of the $DOPC/ACTH_{1-10}$ model membranes in an atmosphere of N_2 saturated with ^2H_2O, the β-pleated sheet structures partially vanished (Figure 2). Contact with liquid H_2O or ^2H_2O led to the complete disappearance of the amide absorption bands, i.e., to a complete escape of the peptide from the membranes.

A plausible interpretation of the observed spectroscopic facts is that the $ACTH_{1-10}$ molecules were not homogeneously distributed within the dry, unequilibrated DOPC membranes but that there were domains in the lipid continuum that contained only $ACTH_{1-10}$ molecules. Within these domains, antiparallel β-pleated sheet structures were predominant. The peptide chains within the pleated sheets were oriented more or less parallel to the DOPC hydrocarbon chains.

In the antiparallel β-pleated sheet structure of $ACTH_{1-10}$, like charges are separated as far as possible from one another, but opposite charges (N and C termini, Glu γ-carboxy, and Arg δ-guanidinium) are very close together. Thus, favorable Coulombic interactions and intermolecular hydrogen bonding could explain the preference for the antiparallel β-pleated sheet of $ACTH_{1-10}$ in the hydrophobic surroundings of a dry model membrane. However, in an aqueous phase, a better stabilization of the $ACTH_{1-10}$ molecules must have been achieved by interaction with the water dipoles. Hence, moistening or equilibration of the dry $DOPC/ACTH_{1-10}$ model membranes with H_2O or ^2H_2O destroyed the β-pleated sheet structures and dissolved the peptide out of its domains in the lipid matrix. The holes thus produced facilitated the transmembrane escape of the peptide through the multiple layers (this was in contrast to the behavior of $ACTH_{1-24}$, see below). Undoubtedly, $ACTH_{1-10}$ preferred the aqueous phase and showed little tendency to become adsorbed to or incorporated into equilibrated DOPC multibilayer membranes.

α-Helix of $ACTH_{1-24}$. The IR-ATR spectra of $ACTH_{1-24}$ deposited as a solvent-free film on the ZnSe plate (Figures 3a and 4) exhibited nonpolarized amide I and II bands, the former with absorption maxima at 1650 cm^{-1}. Position and shape of the amide I absorption (Miyazawa, 1967) and the lack of polarization indicated predominantly random secondary structures of the peptide.

In equilibrated $DOPC/ACTH_{1-24}$ model membranes, the absorption maximum of the amide I band was shifted to 1660 cm^{-1} (Figure 3b,c), Nabedryk-Viala et al. (1978) find a similar amide I absorption at 1657 cm^{-1} for $ACTH_{1-24}$ dissolved in trifluoroethanol, a solvent known to reproduce some of the

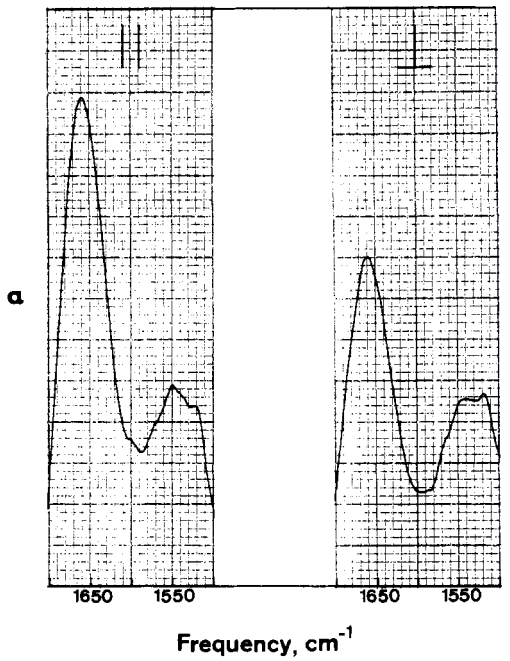

FIGURE 5: Adsorption of $ACTH_{1-24}$ to DOPC bilayers reflected by the amide I and amide II IR-ATR absorption bands (absorbance plot, $\alpha = -\log T$, in which T is transmittance): ($\parallel$ and $\perp$) parallel and perpendicular polarized incident light, respectively. The pure DOPC membrane was contacted with a 0.1 mM solution of $ACTH_{1-24}$ in ^2H_2O for 64 h at 25 °C. Spectra were recorded after flushing and adequate drying of the sample with N_2, 25 °C. Spectra of the pure DOPC bilayer have been subtracted.

effects of membrane surroundings (Pitner & Urry, 1972). From studies with circular dichroism (Greff et al., 1976), Nabedryk-Viala et al. (1978) conclude that, in trifluoroethanol, $ACTH_{1-24}$ contains an α-helix near its N terminus (probably segment 3–9) and that such high wavenumbers are characteristic of α-helices that are strongly constrained by hydrophobic surroundings. Thus, position and shape of the amide I band (Figure 3) indicated the presence of constrained α-helical secondary structures of $ACTH_{1-24}$ in equilibrated DOPC membranes.

As shown in Figure 4, the dichroic ratio of the amide I band of $ACTH_{1-24}$ increased from $R = 1.1$ in the absence of lipid to $R = 1.8$ in fully equilibrated membranes with molar ratios of DOPC/$ACTH_{1-24}$ of 120:1. Simultaneously, the dichroic ratio of the amide II absorption was lowered from $R = 1.0$ to $R = 0.9$. These polarizations indicated that the axes of the α-helical structures were oriented perpendicularly to the membrane surfaces. The increase of polarization with dilution of $ACTH_{1-24}$ in the membranes was tentatively explained by decreased steric hindrance between the $ACTH_{1-24}$ molecules in the membranes.

In order to examine the *adsorption* of $ACTH_{1-24}$ from its aqueous solution, DOPC multibilayers were contacted with a 0.1 mM solution of $ACTH_{1-24}$ in ^2H_2O during 64 h at 25 °C. After removal of excess solution and adequate drying of the membrane in a current of N_2, the peptide spectra shown in Figure 5 were obtained. The amide I band was located at 1660 cm^{-1}, and the dichroic ratios of the amide I and II bands were $R = 1.7$ and $R = 0.9$, respectively. $ACTH_{1-24}$ absorbed to preformed DOPC membranes was thus found to exhibit the same spectroscopic and molecular characteristics as highly diluted $ACTH_{1-24}$ in fully equilibrated membranes (Figure 3b,c).

In films of pure $ACTH_{1-24}$, about 88% of the amide protons were found to be accessible to *deuterium exchange* by equilibration in an atmosphere of N_2 saturated with ^2H_2O for 16 h. This amount was somewhat lower for $ACTH_{1-24}$ in equilibrated membranes with a molar ratio of DOPC/peptide of 100:1. Though the results were not exactly quantified, they are compatible with the idea that a part of the $ACTH_{1-24}$ molecule forms an α-helical structure that enters the lipid bilayers. In support of this hypothesis, labeling experiments with a hydrophobic photomarker reveal that $ACTH_{1-24}$ extends its classical message sequence, amino acids 1–10, into the hydrophobic phase of lipid bilayer vesicles (Schwyzer et al., 1983; B. Gysin and R. Schwyzer, unpublished results). Our model was consistent with the behavior of ACTH peptides in trifluoroethanol (circular dichroism, Greff et al., 1976, and infrared spectroscopy, Nabedryk-Viala et al., 1978) and agreed with the α-helix-forming potential of the segment 3–9 of $ACTH_{1-24}$ calculated by the method of Chou & Fasman (1978).

The value of 0.1 mM $ACTH_{1-24}$ in liquid ^2H_2O used in the absorption experiments was clearly above physiological hormone concentrations. It was needed to produce peptide concentrations in the membrane that could readily be observed in the IR spectra. Such concentrations in the membranes with about 1 molecule of $ACTH_{1-24}$/100–200 lipid molecules are very probably far above the local concentrations needed to produce physiological effects. Furthermore, biological membranes of the adrenal cortex contain about 10% negatively charged lipid (Seltzmann et al., 1974). This causes the surface concentrations of 6-fold positively charged molecules to be increased over the bulk concentration by the Boltzmann distribution factor, $\exp[-zFV_G/(RT)]$, which equals about 1000 at physiological ionic strengths (Gremlich et al., 1981). That means that with biological membranes having such a surface charge, the interactions observable with IR-ATR could already occur in the submicromolar concentration range. Biological membranes are expected to interact with ACTH peptides in a manner similar to that with the model membranes used in our studies, because the unsaturated lipid in fully equilibrated DOPC membranes has a liquid-crystalline ultrastructure (Fringeli, 1977) resembling that of native membranes. Thus, observed conformational and orientational effects may indeed be of potential biological significance.

Transmembrane diffusion experiments gave additional information about the interaction of $ACTH_{1-24}$, especially its C-terminal tetradecapeptide segment, with DOPC multibilayer membranes. No significant loss of peptide was observed upon contacting a fully equilibrated DOPC/$ACTH_{1-24}$ (120:1) membrane system with an aqueous environment at 20 °C up to 24 h. This means that, in contrast to the situation with $ACTH_{1-10}$, the $ACTH_{1-24}$ stuck firmly in and between the bilayers without transgressing them. This behavior was similar to that of alamethicin (Fringeli, 1980). The time constant, τ_0, for the diffusion of this peptide antibiotic across one bilayer membrane critically depends on the electric charge of the alamethicin molecule. Uncharged alamethicin F50 has $\tau_0 = 0.245$ h, whereas alamethicin F30 with one negative charge has $\tau_0 = 2.24$ h. Therefore, $ACTH_{1-24}$ with its net charge of 6+ was not expected to exhibit any significant transmembrane diffusion within 24 h. On the other hand, $ACTH_{1-10}$ has zero net charge, explaining its very rapid escape from the membrane system.

From these experiments, we concluded that, whereas the N-terminal part of $ACTH_{1-24}$ forms an α-helix that enters the DOPC bilayer perpendicularly and is constrained because of its hydrophobic surroundings (strengthening of internal hydrogen bonds), the C-terminal part containing the cluster of positive charges is located between the polar regions of suc-

$$R_z^{ATR} = \frac{A_p}{A_v} = \frac{\sum_{i=1}^{N} x_i m_i^2 \left(E_x^2 \left[S_i \left(\frac{1}{2} \sin^2 \theta_i - \frac{1}{3} \right) + \frac{1}{3} \right] + E_z^2 \left[S_i \left(\cos^2 \theta_i - \frac{1}{3} \right) + \frac{1}{3} \right] \right)}{\sum_{i=1}^{N} x_i m_i^2 E_y^2 \left[S_i \left(\frac{1}{2} \sin^2 \theta_i - \frac{1}{3} \right) + \frac{1}{3} \right]} \quad (1)$$

cessive bilayers and is incapable of penetrating and transgressing the hydrophobic part of the membrane (model in Figure 6). This view is supported by the results of hydrophobic labeling: adrenocorticotropin-(11–24)-tetradecapeptide ($ACTH_{11-24}$) is not labeled by lipid bilayer vesicles containing a hydrophobic photomarker, and in $ACTH_{1-24}$, only the segment 1–10 is labeled (Schwyzer et al., 1983; B. Gysin and R. Schwyzer, unpublished results).

Quantitative Evaluation of Dichroic Ratios Observed for $ACTH_{1-24}$. We finally had to examine the consistency between our proposed model (Figure 6) and the observed dichroic ratios (Figure 4). For a system with liquid-crystalline ultrastructure and molecular orientation along the z axis (normal to the ZnSe plate), the analytical dependence of the dichroic ratio R on distinct functional groups with uniform mean conformation is derived for ATR spectroscopy by Fringeli (1977). The expression was now generalized for the case where equal functional groups of a molecule may assume N different conformations with relative fractions x_i ($\sum_{i=1}^{N} x_i = 1$) and relative magnitudes $m_i = M_i/M_1$ of the corresponding transition dipole moments M_i. If S_i denotes the order parameter of the ith segment and θ_i the angle between equal functional groups of the ith segment and the molecular axis, straightforward derivation is as shown in eq 1 wherein E_x, E_y, and E_z denote the components of the electric field of the ATR beam in the rarer medium (Fringeli, 1977; Fringeli & Günthard, 1981).

In our case of $ACTH_{1-24}$, the number N of different segments is at least 2. Assuming one segment (1) to comprise the N-terminal amino acids 1–10 and the other segment (2) the C-terminal amino acids 11–24, we obtained $x_1 = 0.42$ and $x_2 = 0.58$, respectively. Furthermore, S_1 (of segment 1) was estimated from the hydrocarbon chain ordering in the DOPC multibilayer: Figure 4 shows that the dichroic ratio of the rocking vibration of the CH_2 groups, $\gamma_r(CH_2)$, is not significantly affected by the interaction with $ACTH_{1-24}$. If one assumes the hydrocarbon chains to be oriented perpendicularly to the ATR plate, the observed dichroic ratio resulted in an order parameter of 0.4. This value is consistent with NMR data published by Seelig & Waespe-Šarčevič (1978). If we assumed an order parameter of the same magnitude for the α-helical part of $ACTH_{1-24}$ (amino acids 1–10, $x_1 = 0.42$) that was incorporated into the membrane, we had to conclude from the dichroic ratio of the amide I band that the segment in the polar region between the bilayers (2, amino acids 11–24, $x_2 = 0.58$) is also considerably ordered.[2] Calculation from eq 1 with $R = 1.8$ yielded an order parameter $S_2 = 0.5$–0.6 for that part of the molecule. A possible explanation of such an ordering effect was the assumption of distinct electrostatic interactions between charged side chains of the peptide segment (particularly Lys and Arg) and polar head groups (phosphatidylcholine) of the membrane surface. Such interactions could have resulted in different, more or less extended chain conformations in which the planes of peptide bonds were about perpendicular to the membrane surface (Figure 6). Of course, the order parameter of this segment could be considerably lower, if the order parameter of the α-helical segment proved to be higher than that of the hydrocarbon chains, which is perhaps not unreasonable.

Conclusions and Projections

The potent steroidogenic full agonist $ACTH_{1-24}$ is present as a predominantly random structure in aqueous solution (Greff et al., 1976) and in solvent-free films on the ZnSe crystals used in our IR-ATR studies. On contact with bilayer membranes prepared from DOPC, the peptide is adsorbed from the aqueous solution to the lipid membrane. The adsorption is accompanied by a conformational transition that is similar to that observed with trifluoroethanol (Greff et al., 1976; Nabedryk-Viala et al., 1978), a solvent mimicking effects of lipid membranes (Pitner & Urry, 1972).

This conformational transition is particularly pronounced at low peptide/lipid molar ratios (e.g., 1:120). The most prominent feature is the transition of all or part of the N-terminal segment (between amino acids 1–10) from a random to an α-helical secondary structure. This portion of the molecule [that is known to contain the structural elements necessary for triggering steroidogenic, melanotropic, and central nervous receptors; see Schwyzer (1977)] is embedded into the membrane (Schwyzer et al., 1983).

Probably because of the liquid-crystalline ultrastructure of the membrane, the axes of the molecular helices become arranged perpendicularly to the membrane surface and stand roughly parallel to the lipid hydrocarbon chains (Figure 6). A conformational transition of the C-terminal segment [amino acids 11–24, known to potentiate the action of the segment 1–10 on steroidogenic receptors; see Schwyzer (1977)] is less well-defined. Segment 11–24 remains on the hydrophilic surface of the lipid membranes (Schwyzer et al., 1983), but according to our calculations from the observed dichroic ratios, some of its peptide bonds appear to be preferentially oriented perpendicularly to the membrane surface. Such preferred orientations are possible even for otherwise irregular secondary structures (without regular repeat of ϕ, ψ, and ω angles) if the side chains of the amino acids containing polar functional groups (e.g., Lys and Arg in our case) interact with the hydrophilic head group layer of the membrane, thus causing the segment to lie more or less flat on the membrane surface (Figure 6).[2]

Without the covalently attached C-terminal segment 11–24, the peptide $ACTH_{1-10}$ behaves very differently. As a solid on the ZnSe crystal, it contains random and antiparallel β-pleated sheet secondary structures. It shows no tendency to be adsorbed to DOPC membranes from aqueous solutions. If it is forced into dry DOPC membranes (by evaporation of methanolic solutions of lipid plus peptide), rigid antiparallel β-pleated sheet structures are observed. They are more pronounced the higher the peptide/DOPC molar ratio. The β-pleated sheet structures appear to be clustered into domains, in which the fiber axes stand parallel to the lipid hydrocarbon chains. Upon contact with water, the peptide very quickly

[2] IR-ATR spectroscopy revealed that $ACTH_{11-24}$ assumed an irregular extended structure in the aqueous layers between the equilibrated membranes (^1H–^2H exchange). This structure was characterized by a perpendicular orientation of the peptide bonds, as observed for the corresponding segment in $ACTH_{1-24}$. The tetradecapeptide was not measurably adsorbed to preformed membranes from 0.1 mM solutions, stressing the importance of hydrophobic interactions for the adsorption of $ACTH_{1-24}$. Once incorporated into equilibrated membranes, it was not removed by washing, in agreement with its strong positive charge (H.-U. Gremlich et al., unpublished results).

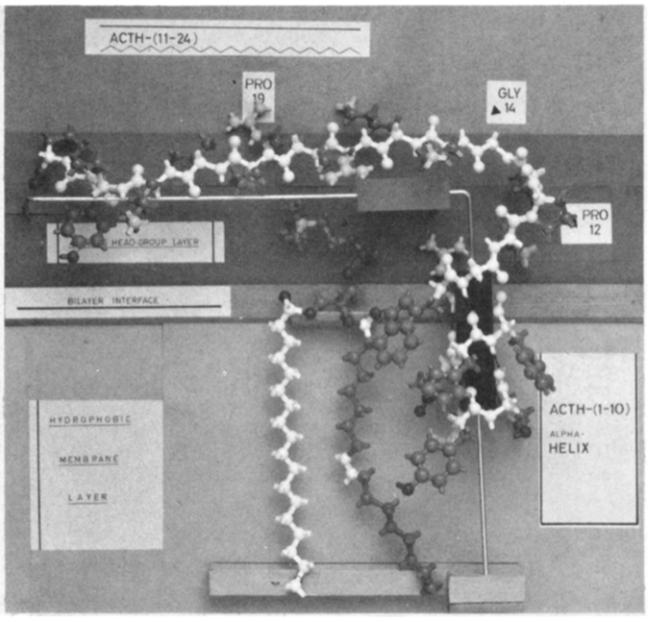

FIGURE 6: Model illustrating the interaction of $ACTH_{1-24}$ with lipid membranes.

escapes from the lipid environment, again in contrast to the behavior of $ACTH_{1-24}$.

Probably the most interesting conclusion from our observations is the one pertaining to the role of the peptide segment 11–24. This segment, which is known drastically to potentiate the steroidogenic effect of the segment 1–10 and to permit it to perform its ACTH-specific hormonal effects in the adrenal cortex, also permits the observed random coil → α-helix transition of the receptor-triggering segment 1–10 and its entry into the lipid phase in a topologically defined manner. Without it, segment 1–10 does not interact with DOPC membranes in aqueous surroundings; with it, it sticks firmly in the membranes. This influence of the strongly charged, hydrophilic address segment on the behavior of the more hydrophobic message segment is consistent with current ideas about the role of charge clusters in the orientation of membrane proteins (Weinstein et al., 1982). A similar influence of a charged address segment is found in dynorphin (Schwyzer et al., 1983; Gysin & Schwyzer, 1983).

The preference of $ACTH_{1-10}$ for the aqueous phase and for the antiparallel β-pleated sheet structure in hydrophobic surroundings may provide an explanation for its very low potency in some biological systems and for its rather high potency in others. We can speculate that a lipid interaction and/or a helical structure of the receptor-triggering moiety ("message") aids in, or is even necessary for, a productive reaction with steroidogenic receptors of the adrenal cortex but is less essential for the activation of neuronal receptors of the central nervous system [see Schwyzer (1977)]. The latter could, for example, have their hormone-recognition sites exposed on the hydrophilic surface of the membrane, and these sites might be able to recognize a secondary structure more closely related to the antiparallel β-pleated sheet. Thus, $ACTH_{1-10}$ would be a potent agonist for this type of receptor. On the other hand, the steroidogenic receptors might have their hormone-recognition sites more exposed to the hydrophobic layer of the membrane, and these sites might prefer an α-helical structure of the receptor-triggering peptide segment. Thus, $ACTH_{1-24}$ would be a particularly potent agonist for such receptors.

In summary, the lipid phase of the target-cell surface may not only serve as a matrix for the correct orientation and folding of the receptor proteins but also facilitate the correct orientation and folding of the peptide hormones prior to their receptor contact. The apparent difference in topological requirements of receptors for different functions of one and the same hormone possibly also applies to μ, δ, and κ receptors for enkephalins and endorphins (Schwyzer et al., 1983; Gysin & Schwyzer, 1983).

Acknowledgments

We thank Prof. Dr. K. Mühlethaler (Institut für Zellbiologie der Eidgenössischen Technischen Hochschule Zürich) for the generous permission to use his infrared spectrometer.

Registry No. DOPC, 4235-95-4; $ACTH_{1-10}$, 2791-05-1; $ACTH_{1-24}$, 16960-16-0.

References

Adam, G., & Delbrück, M. (1968) in *Structural Chemistry and Molecular Biology* (Rich, A., & Davidson, N., Eds.) pp 198–215, W. H. Freeman, San Francisco.

Berg, H. C., & Purcell, E. M. (1977) *Biophys. J. 20*, 193–219.

Chirgadze, Y. U. N., & Nevskaya, N. A. (1976) *Biopolymers 15*, 607–625.

Chou, P. Y., & Fasman, G. (1978) *Annu. Rev. Biochem. 47*, 251–276.

de Wied, D., Witter, A., & Greven, H. M. (1975) *Biochem. Pharmacol. 24*, 1463–1468.

Eberle, A., & Schwyzer, R. (1976) *NATO Adv. Study Inst. Ser., Ser. A 12*, 291–304.

Fringeli, U.-P. (1977) *Z. Naturforsch., C: Biosci. 32C*, 20–45.

Fringeli, U.-P. (1980) *J. Membr. Biol. 54*, 203–212.

Fringeli, U.-P., & Günthard, H. H. (1981) in *Membrane Spectroscopy* (Grell, E., Ed.) pp 270–332, Springer Verlag, Berlin and Heidelberg, West Germany.

Greff, D., Thoma, F., Fermandjian, S., Löw, M., & Kisfaludy, L. (1976) *Biochim. Biophys. Acta 439*, 219–231.

Gremlich, H.-U., Sargent, D. F., & Schwyzer, R. (1981) *Biophys. Struct. Mech. 8*, 61–65.

Gysin, B., & Schwyzer, R. (1983) *Arch. Biochem. Biophys.* (in press).

Harrick, N. J. (1967) *Internal Reflection Spectroscopy*, Interscience, New York.

Lang, U., Karlaganis, G., Vogel, R., & Schwyzer, R. (1974) *Biochemistry 13*, 2626–2633.

Miyazawa, T. (1967) *Biol. Macromol. 1*, 69–103.

Nabedryk-Viala, E., Thiery, C., Calvet, P., Fermandjian, S., Kisfaludy, L., & Thiery, J. M. (1978) *Biochim. Biophys. Acta 536*, 252–262.

Nevskaya, N. A., & Chirgadze, Y. U. N. (1976) *Biopolymers 15*, 637–648.

Pitner, T. P., & Urry, D. W. (1972) *J. Am. Chem. Soc. 94*, 1399–1400.

Schulster, D., & Schwyzer, R. (1980) in *Cellular Receptors for Hormones and Neurotransmitters* (Schulster, D., & Levitzki, A., Eds.) pp 197–207, Wiley, New York.

Schwyzer, R. (1977) *Ann. N.Y. Acad. Sci. 297*, 3–26.

Schwyzer, R. (1982) *Naturwissenschaften 69*, 15–20.

Schwyzer, R., & Kappeler, H. (1963) *Helv. Chim. Acta 46*, 1550–1572.

Schwyzer, R., Rittel, W., Kappeler, H., & Iselin, B. (1960) *Angew. Chem. 72*, 915–917.

Schwyzer, R., Schiller, P., Seelig, S., & Sayers, G. (1971) *FEBS Lett. 19*, 229–231.

Schwyzer, R., Gremlich, H.-U., Gysin, B., & Fringeli, U. P. (1983) in *Peptides 1982* (Blaha, K., & Malon, P., Eds.) pp

55-71, de Gruyter, Berlin and New York.
Seelig, J., & Waespe-Šarčevič, N. (1978) *Biochemistry 17*, 3310-3315.
Seelig, S., Sayers, G., Schwyzer, R., & Schiller, P. (1971) *FEBS Lett. 19*, 232-234.
Seltzmann, T. P., Finn, F. M., Widnell, C. C., & Hofmann, K. (1974) *J. Biol. Chem. 250*, 1193-1196.
Sonenberg, M., & Schneider, A. S. (1977) *Recept. Recognition, Ser. A 4*, 1-73.
Squire, P. G., & Bewley, T. (1965) *Biochim. Biophys. Acta 109*, 234-240.
Toma, F., Dive, V., Lam-Than, H., Piriou, F., Lintner, K., Fermandjian, S., Low, M., & Kisfaludy, L. (1981) *Biochimie 63*, 907-910.
Weinstein, J. N., Blumenthal, R., van Renswoude, J., Kempf, C., & Klausner, R. D. (1982) *J. Membr. Biol. 66*, 203-212.

Nerve Growth Factor Synthesized by Mouse Fibroblast Cells in Culture: Absence of α and γ Subunits†

Nicholas J. Pantazis

ABSTRACT: Nerve growth factor (NGF) is found in high concentrations in the mouse salivary gland. However, this gland is unique since salivary glands from other animals have only trace amounts of NGF. In the mouse gland, two high molecular weight forms of NGF have been reported, 7S-NGF [Varon, S., Nomura, J., & Shooter, E. M. (1967) *Biochemistry 6*, 2202-2209] and NGF_1 [Young, M., Saide, J. D., Murphy, R. A., & Blanchard, M. H. (1978) *Biochemistry 17*, 1490-1498]. 7S-NGF is comprised of three noncovalently associated subunits: β-NGF, which is the biologically active subunit, α subunit, and γ subunit. A similar subunit composition is seen with NGF_1 (unpublished work with R. A. Murphy). Since the mouse salivary gland is unique with regard to its synthesis of NGF, the following question arises. Do other sources of NGF produce either 7S-NGF or NGF_1? Mouse fibroblast cells (L_{929}) in culture synthesize and secrete into their feeding medium (conditioned medium) a β-NGF-like molecule [Pantazis, N. J., Blanchard, M. H., Arnason, B. G. W., & Young, M. (1977) *Proc. Natl. Acad. Sci. U.S.A. 74*, 1492-1496]. These cells therefore provided the opportunity to examine the molecular nature of NGF produced by a nonsalivary gland source. In this study, it was determined by radioimmunoassay that neither the α nor the γ subunit is present in fibroblast cell conditioned medium. Since α- and γ-proteins are present in both 7S-NGF and NGF_1, this indicates that neither of the salivary gland forms of NGF are produced by the mouse fibroblast cell.

The biochemical and biological properties of nerve growth factor (NGF)[1] in the mouse submandibular gland have been studied extensively. Two high molecular weight forms of NGF called 7S-NGF (Varon et al., 1967) and NGF_1 (Young et al., 1978) have been isolated from this tissue by using different purification protocols. The 7S-NGF complex (molecular weight, M_r, 130000) contains three noncovalently associated protein subunits called α, γ, and β-NGF. Only the β-NGF subunit is capable of producing the NGF biological response which is stimulation of neurite outgrowth from sensory and sympathetic ganglia. β-NGF elicits neurite formation at concentrations of 10 ng/mL. The α subunit has no known function. It has been suggested that the γ subunit is involved in cleavage of a pro-β-NGF precursor to produce β-NGF (Berger & Shooter, 1977).

The α, γ, and β-NGF subunits of 7S-NGF are noncovalently associated and will dissociate from one another when the 7S-NGF complex is diluted to biologically active concentrations (Pantazis et al., 1977b). This observation has been corroborated by the demonstration that 7S-NGF must dissociate in order for the β-NGF molecule to bind to NGF receptors (Harris-Warrick et al., 1980). The binding of β-NGF to its receptors is probably the initial step in the NGF biological response.

Recent isoelectric focusing experiments with NGF_1 (M_r 116000) indicate that this complex contains proteins with isoelectric points similar to those found in 7S-NGF (unpublished work with R. A. Murphy). These electrophoretic results suggest that NGF_1, like 7S-NGF, contains α, γ, and β-NGF.

Both 7S-NGF and NGF_1 are purified from the mouse submandibular gland. However, this source of NGF is unique in that most other animals do not have high concentrations of NGF in their salivary glands (Levi-Montalcini & Angeletti, 1968). Since NGF is known to play a vital role in neuronal development and maintenance in many species, where does the NGF come from? There is the possibility that several different types of tissues synthesize small quantities of NGF to maintain the peripheral nervous systems in the animal. Trace amounts of NGF have been reported in several tissues (Bueker et al., 1960; Levi-Montalcini et al., 1954;) however, the NGF in these tissues has not been biochemically characterized because of the low concentrations. Further support for the concept of multisite synthesis of NGF is the fact that several different cell types in culture synthesize NGF (Oger et al., 1974; Young et al., 1975; Longo & Penhoet, 1974; Murphy et al., 1975, 1977a,b; Pantazis et al., 1977a) and

† From the Department of Anatomy, University of Iowa, Iowa City, Iowa 52242. *Received February 22, 1983.* This work was supported by a grant from the National Institutes of Health (General Medical Sciences Grant GM 28644) and by a grant from the Lindsay Trust.

[1] Abbreviations: NGF, nerve growth factor; LCM, L cell conditioned medium; BSA, bovine serum albumin; M_r, molecular weight; EDTA, ethylenediaminetetraacetic acid; DE-52, diethylaminoethylcellulose; CM-52, carboxymethylcellulose; IEF gels, isoelectric focusing gels; RIA, radioimmunoassay; D-MEM, Dulbecco's modified Eagle's medium; IgG, γ-globulin.

0006-2960/83/0422-4264$01.50/0